JOURNAL OF APPLIED POLYMER SCIENCE VOL. 20, 2691–2704 (1976)

Structure and Properties of ABS Polymers. X. Influence of Particle Size and Graft Structure on Loss Modulus Temperature Dependence and Deformation Behavior*

L. MORBITZER, D. KRANZ, G. HUMME, and K. H. OTT, *Bayer AG, Leverkusen, Germany*

Synopsis

ABS systems which differ distinctly in particle size and degree of grafting were prepared and investigated by dynamic mechanical measurements as function of temperature in the glass transition region of the rubber phase. Variation of rubber content within different sample series results in effects which were mainly referred to thermal stresses as consequence of phase interactions. Basic aspects of the deformation behavior of some of these ABS systems are studied by mechanical and morphological methods, and the operation modes of the component of a bimodal/bigraft-system concerning toughness are discussed.

INTRODUCTION

Many investigations in the field of ABS have shown that particle size and graft structure are dominating factors controlling many important properties.[1–5] Recent developments describe ABS systems using combinations of rubbers with different particle size.[2,3] Beyond this, mixtures of grafts with different particle size and additionally changed degrees of grafting can result in improved properties, i.e., impact, gloss, and processing, compared with standard ABS types. These bimodal/bigraft systems exhibit a number of problems which demand further physical investigations.

The importance of good interfacial bonding between rubber particle and SAN surrounding is always emphasized, but in the literature there is a lack of experimental evidence for describing these effects in bulk material.

The first part of the present paper deals with some aspects concerning interfacial bonding using the well-known fact that thermal stresses arise in ABS systems when samples are cooled down from the melt or from ambient temperatures influencing thereby the glass transition of the rubber phase by volume dilatations of the rubber particles.[6–9] In the second part, remarks are made about the resulting deformation behavior comparing notched impact values and the morphology of the fracture surfaces gained at high and low strain rates. In addition, fracture phenomena from slow penetration tests and transmission electron micrographs from the notched impact material are presented.

* Presented at IUPAC Symposium, Madrid, Spain, 1974.

MATERIALS

Different series of samples were prepared by mixing emulsion-grafted rubber with SAN resin: the first with small particles and a high degree of grafting (SPHG), the second with large particles and also with a high degree of grafting (LPHG), the third with large particles but a lower degree of grafting (LPLG), and the fourth a mixture of SPHG and LPLG with a S/L ratio of 1:1. In each of these series, the rubber content was varied up to a maximum content of 30%. The grafting degree of the SPHG and LPHG series was about 0.5–0.8, and of the LPLG series less than 0.5. The S/AN ratio was usually 75/25. Only for the LPLG series was the AN content of the graft somewhat lower than that of the matrix. The fifth series contained samples of constant rubber level but different S/L ratios. Finally, the sixth series was built up with small particles but different degrees of grafting (SPDG), where again the total rubber content was constant. Thin sheets (1 mm thick) were prepared by compression molding.

RESULTS AND DISCUSSION

Phase Interactions

For characterizing phase interactions, we measured the temperature dependence of shear modulus with a torsional pendulum at a frequency of about 1 Hz. The two components of the ABS systems show distinct glass transitions: one, in the region of about −80°C, belongs to the rubber phase (polybutadiene), and the other, in the region of about +100°C, belongs to the SAN phase. In the following, we will only look at the glass transition of the rubber phase which is represented by plots of the loss modulus as function of reciprocal temperature in the glass transition region of the rubber phase.

Prior to the measurements, the samples were annealed at 130°C for 1 hr and then slowly cooled down to room temperature. In the thermostat of the torsional pendulum, the samples were cooled down to −180°C at a rate of 10°/min, and then for measuring heated up at a mean rate of 1°/min. Between the annealing procedure and the pendulum measurements, an always constant time difference was observed.

Figure 1 gives the G''-versus-$1/T$ plot for the SPHG series (the G'' scale holds for the bottom curve; the other curves are shifted upward by certain amounts). Increasing rubber content causes an increasing G'' maximum, as expected. Simultaneously, a shift of the peak temperature is to be observed to lower temperatures with decreasing rubber content. This shift refers not only to the peak temperature but to the maximum on the whole.

Influences of rubber phase content on E'' and tan δ were recently discussed in the literature,[10] where the shift of E'' and tan δ to lower peak temperatures with lowered rubber content was explained by an apparent diminished width of the rubber glass transition. In the present case, it seems to us not possible to interpret the observed shifts only with the explanation given in reference 10. Beyond this, we refer the influence of decreasing rubber content mainly to increased thermal stresses caused by an increased modulus of the surrounding of a single rubber particle and a greater difference in thermal expansion between rubber particle and surrounding. The stress fields around

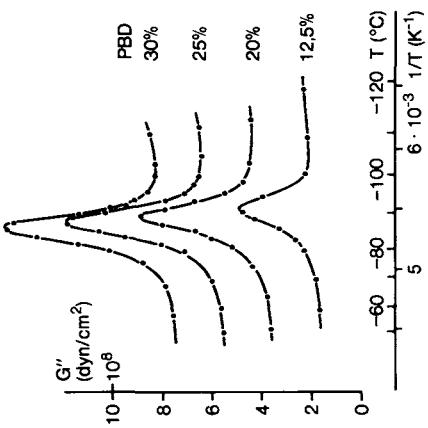

Fig. 1. Loss modulus for the small-particle, high-graft series (SPHG).

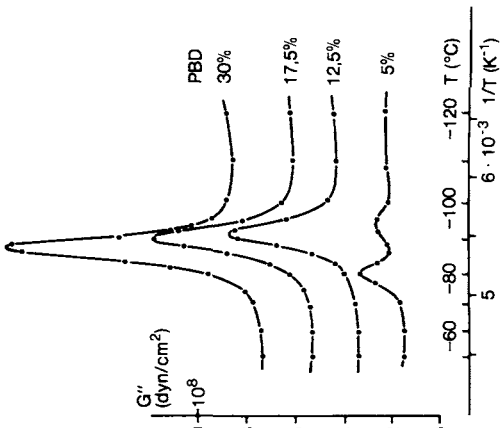

Fig. 2. Loss modulus for the large-particle, high-graft series (LPHG).

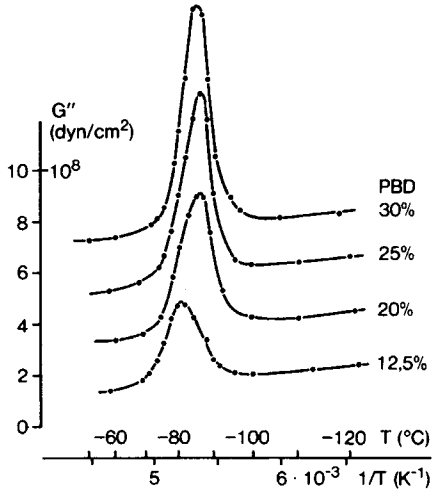

Fig. 3. Loss modulus for the large-particle, low-graft series (LPLG).

the particles overlap as function of rubber content and of the statistical arrangement of the particles, too. An important condition for the influence on T_g of the rubber phase is that the arising stresses are always lower than the adhesion between rubber particle and SAN matrix. We obtained the same results as shown in Figure 1 with the LPHG series given in Figure 2. But, at a very low rubber content, we surprisingly find two G'' maxima, one at a lower temperature than the 12.5% sample, and the other at the temperature where one usually finds the ungrafted rubber phase.[9] This effect can be explained by the assumption of a distribution of grafting degrees: at the low rubber content, the thermal stresses overcome the adhesion of that part of the rubber particles with a smaller grafting degree so that a breakdown of the interfacial bonding will occur with the result of canceling the volume dilatation and therefore the influence on the rubber glass transition.

If the given explanations are true, lowering the grafting degree will cause the described break-off effect to occur at lower thermal stresses, that is, at a

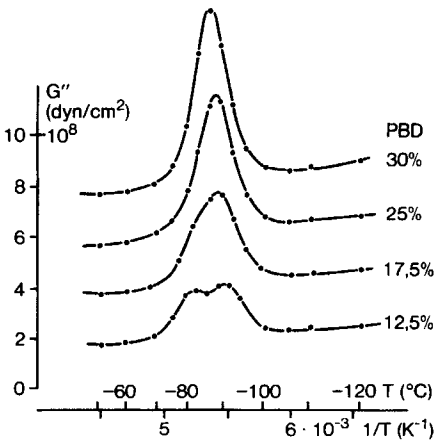

Fig. 4. Loss modulus for the mixed series (SPHG/LPLG) with S/L = 1:1.

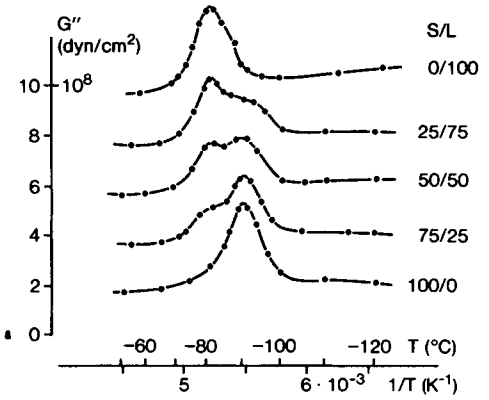

Fig. 5. Loss modulus for different S/L ratios (total rubber content 12.5%).

higher rubber content, compared with that of Figures 1 and 2. As proof for this, we can use the results of the LPLG series shown in Figure 3: the G'' peak of the 12.5% sample is shifted to a temperature which is higher than that of the 30% sample and which nearly coincides with the T_g of the ungrafted rubber phase. This means that, again, a breakdown of the interfacial bonding has occurred. The 20% sample shows a slight shoulder on the high-temperature side of the G'' maximum, which is a sign for the beginning of the interfacial breakdown and for the existence of a distribution of grafting degrees.

For cancelling the thermal stresses around the rubber particles, it seems not to be necessary that the breakdown happens simultaneously and uniformly in the phase boundary; it can be restricted to areas of weakest grafting. Further, it must be stated that scission effects inside the rubber particles will have the same effect on T_g so that the degree of crosslinking of the rubber phase and the breaking parameters become very important. Corresponding experiments with varied crosslink density of the rubber phase are in

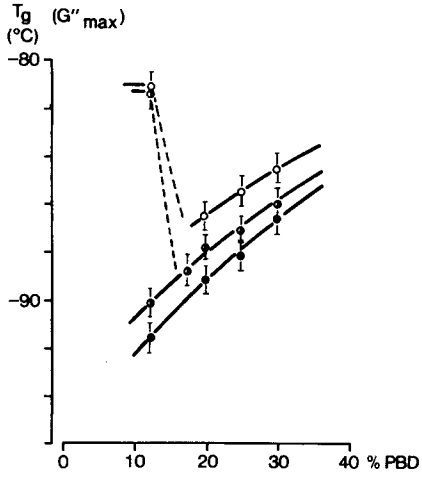

Fig. 6. T_g as function of rubber content for (○) LPLG, (◑) SPHG/LPLG, and (●) SPHG.

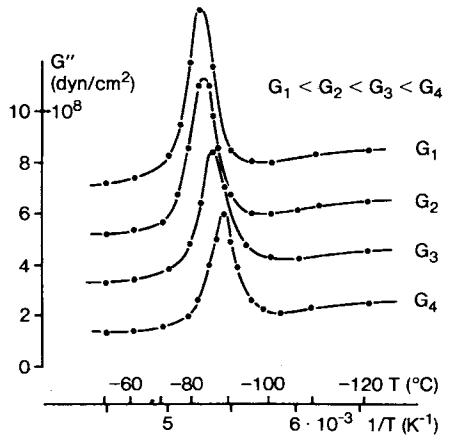

Fig. 7. Loss modulus for the small-particle, different graft series (SPDG); rubber content 17.5%.

preparation. In the present case, we believe that the interfacial bonding strength is mainly responsible for the observed effects.

Figure 4 gives the results for the SPHG/LPLG series. Here, at the lowest rubber content, we find two distinct G'' maxima which can now be related to the two different grafting degrees; the one at the lower temperature belongs to the small-particle/high-grafted component, the other, to the large-particle/low-grafted component, again at the temperature of the ungrafted rubber phase. The 17.5% sample shows a slight shoulder on the high-temperature side of the G'' maximum, similar to that of the 20% sample in Figure 3. At constant rubber level but different S/L ratios, one can observe again the described break-off effect (see Fig. 5), and the changing of the magnitude of the two peaks is in good accordance with the S/L ratios. This is a proof that the break-off effect is a function only of the total rubber content and not of the content of the low-graft component. In addition, DSC measurements were performed, and the observed T_g shifts were qualitatively and in part also

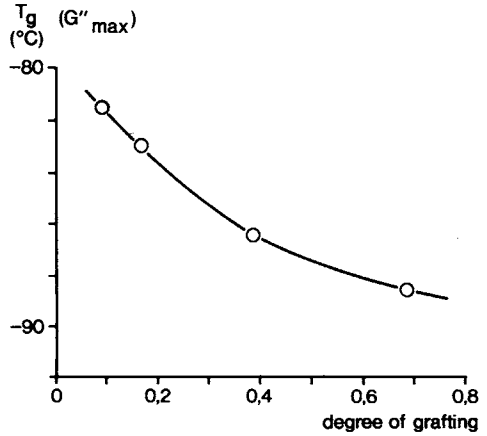

Fig. 8. T_g of the rubber phase as function of grafting degree for the SPDG series.

quantitatively in good agreement with the G'' measurements plotted in Figure 1, 3, and 4.

Figure 6 gives plots of the T_g values (G'' peak temperature) versus rubber content for the SPHG, LPLG, and the SPHG/LPLG series. We find three different curves. The curve for the LPHG series is identical with that of the SPHG series, as one would expect. In total, the LPLG series gives smaller T_g shifts with respect to the ungrafted rubber phase than the SPHG series. The mixed series is in the middle. Probably, a further decrease in rubber content in the SPHG series would produce the same result as in the LPHG series (see Fig. 2).

Finally, Figure 7 shows the result of the SPDG series where the rubber content was kept constant at 17.5%. Increasing degree of grafting indicates a continuous shift of the G'' peak to lower temperatures as consequence of improved interfacial bonding. The observed T_g values as function of grafting degree are plotted in Figure 8. One finds a nearly linear decrease in the beginning which flattens at higher grafting degrees. Again, this is in good accordance with the above discussed result where the rubber content was changed within the different series.

Summarizing the above results, one can see that by varying the rubber content it should be possible to estimate interfacial bonding strength even in the bulk material as function of the grafting and crosslinking parameters, at least in relation one with another.

Deformation Behavior

Deformation and fracture behavior of rubber-toughened plastics is a topic of many papers in the literature (see, for example, ref. 14) so that the miscellaneous ideas need not be repeated here. The following basic concept has been established: the rubber particles act as stress raisers and cause the initiation of numerous crazes more or less simultaneously in a larger portion of the mechanically strained sample volume. These crazes propagate further into the matrix material and are often stopped by other rubber particles before they transform into a crack. In the state of craze propagation, the interfacial bonding between particle and surrounding plays an important role in sustaining triaxial tension and delaying by this the craze–crack transition. Craze initiation is governed by the structure of the phase boundary which can be influenced by the grafting parameters and also by thermal pretreatment.[11] The phase boundary is to be characterized by a local transition in free-volume concentration and may have a variable extension. But also shear yielding is part of the deformation process,[12,13] and further investigations of ABS systems must aim to quantify more exactly the different dependences of the two deformation modes on many parameters.

Both material and loading parameters are responsible for deformation and fracture. In the present case, the samples of the mixed series (SPHG/LPLG) reach higher notched impact values as function of rubber content than the SPHG and LPLG series, as is shown in Figure 9. At about 6% rubber, the three curves reach the impact level of the pure resin. The values of the small particle-size material are much lower than those of the other materials, as is generally known. The temperature dependence is indicated in Figure 10 at

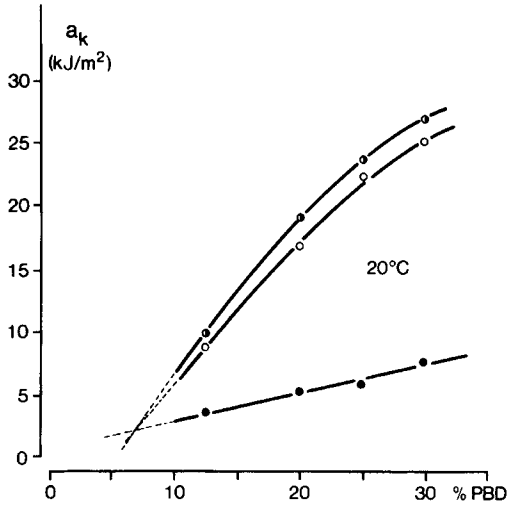

Fig. 9. Notched impact strength as function of rubber content for (○) LPLG, (◑) SPHG/LPLG, and (●) SPHG.

two constant rubber levels. Here, we find for the LPLG material a rapid drop of the impact values below room temperature, reaching almost the curve of the SPHG samples. In comparison with this, the SPHG/LPLG material falls off less rapidly and preserves a considerable amount of toughness even at low temperatures. The impact level of the pure resin is reached by all curves at about −80°C; this is the glass transition region of the used rubber phase.

Photographs of the fracture surfaces produced in notched impact tests at room temperature are seen in Figure 11. Different extents of stress whitening can be observed caused by different grades of craze initiation and propagation. The SPHG material at low rubber content gives only a very faint indication of crazing in the region of the notch tip, and the state of craze propa-

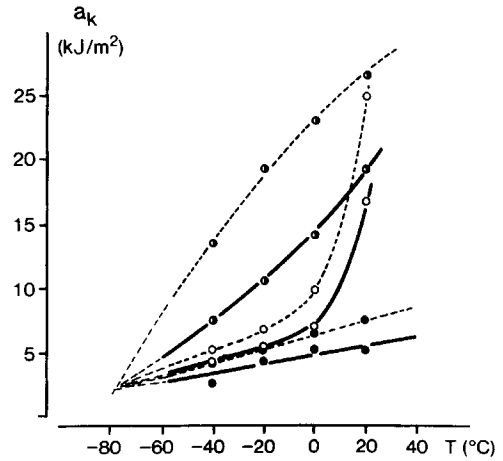

Fig. 10. Notched impact strength as function of temperature for (○) LPLG, (◑) SPHG/LPLG, and (●) SPHG; (- - -) 30% PBD; (—) 20% PBD.

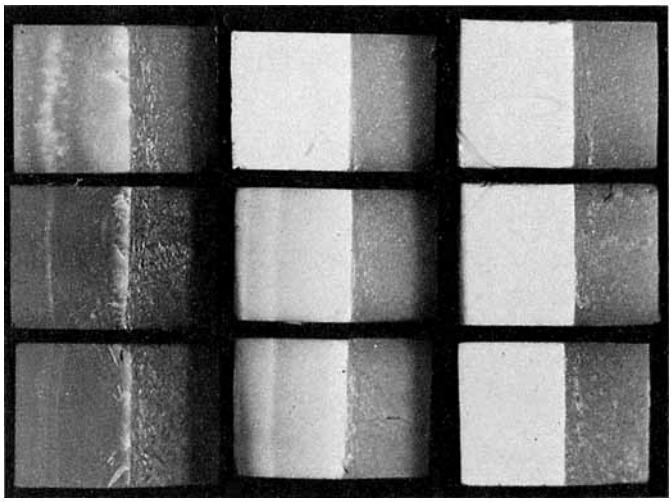

Fig. 11. Photographs of the fracture surfaces (notched, high strain rate). Rubber content 30% (top), 20% (middle), 12.5% (bottom); SPHG (left), LPLG (middle), SPHG/LPLG (right).

gation is quickly relieved by crack initiation so that the residual area of the fracture surface does not show any stress whitening. At higher rubber levels, craze propagation is somewhat increased. At 12.5% rubber, the LPLG material shows much more stress whitening, but not over the whole area. The rapid falloff in toughness at lower temperatures can be explained by the former described breakdown of interfacial bonding which may be enhanced by the mechanical straining due to the multiaxial stress field in the surrounding of a rubber particle. The samples of the SPHG/LPLG series exhibit marked stress whitening over the whole fracture surface even at the low rubber content. Deformation at low strain rates shows stress whitening to almost the same extent for each sample of Figure 10.

More details are seen upon SEM investigation of the fracture surfaces. Figure 12 shows pictures of samples with 12.5% rubber (see bottom line in Fig. 11). The SPHG sample shows a granular structure which may be connected with the size and the arrangement of the small particles. Also, the LPLG sample reveals a structure where one can anticipate that larger particles are involved which probably are pulled out of the surrounding resin. Only the mixed sample shows a fracture surface with the typical yield flow pattern of a fully crazed material. Figure 13 gives once more SEM pictures from the fracture surfaces of the three materials, but now obtained at a low strain rate. Each of these samples indicates a flow pattern similar to that of the mixed sample at high strain rate; in addition, characteristic features concerning particle size are visible.

Complementary to the notched impact examinations, fracture phenomena from penetration tests of thin sheets were achieved at low and high strain rates, as indicated in Figure 14. The pictures are photographs from the highly strained region taken in transmission. All samples contain 17.5% rubber. The shadowed regions are areas of stress whitening. At low strain rate, the SPHG sample shows, at this deformation mode, only a very faint whitening, but exhibits a tough behavior quite comparable to the materials which show

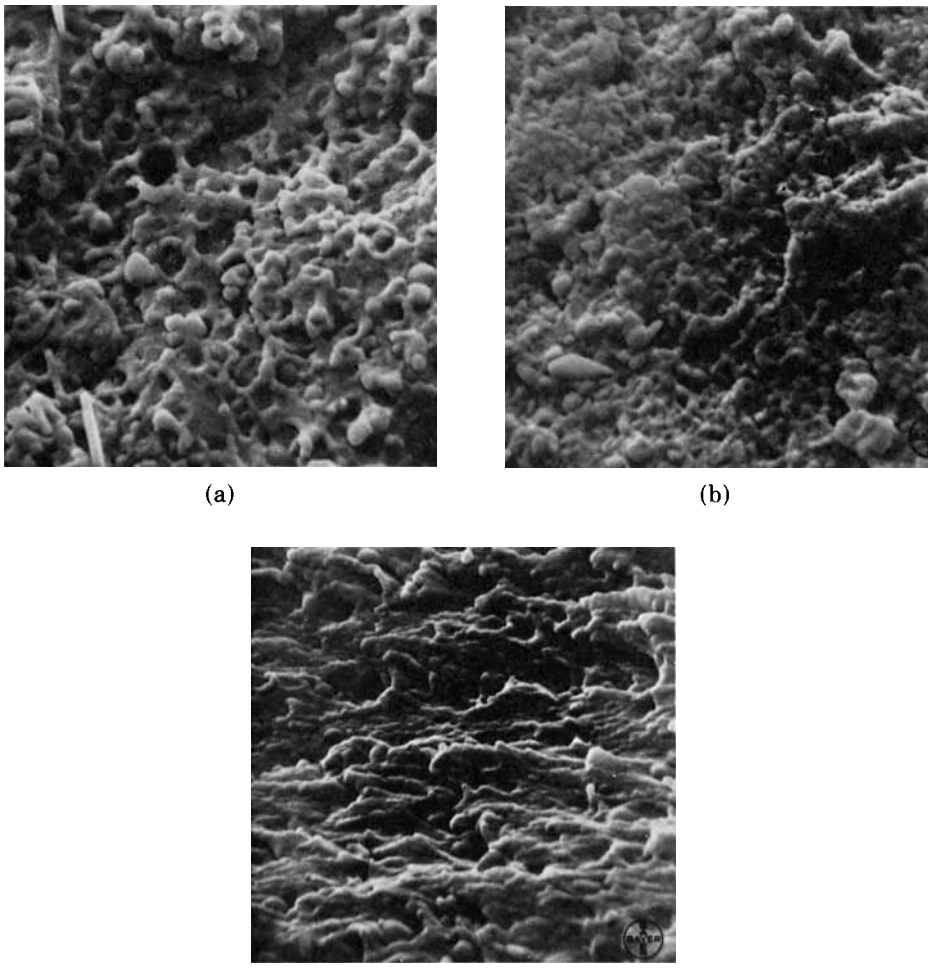

Fig. 12. Scanning electron micrographs from the fracture surfaces (notched, high strain rate). Rubber content 12.5%; SPHG (a), LPLG (b), SPHG/LPLG (c). Magnification 5000×.

pronounced stress-whitened zones. For the mixed sample, this shadowed zone is something smaller, indicating that the extent of crazing should be smaller than for the LPLG material. At high strain rate, the SPHG materials are very brittle, as known from the notched impact tests; the other two materials preserve their toughness recognizable by the stress-whitened zones. Again, the extent of this zone is somewhat smaller for the mixed sample. In both cases, these zones are shadowed more homogeneously than at low strain rates where single craze bands in the radial direction are distinguishable.

During the slow penetration tests, the force–deformation curves with intermittent recycling were registered and are shown in Figure 15. In the beginning, the force increases linearly up to the yield process. The further increase is somewhat flattened until a kind of strain hardening occurs which finally is released by crack initiation. The intermittent recycling results in hysteresis loops with a gradual changing from the SPHG material to the

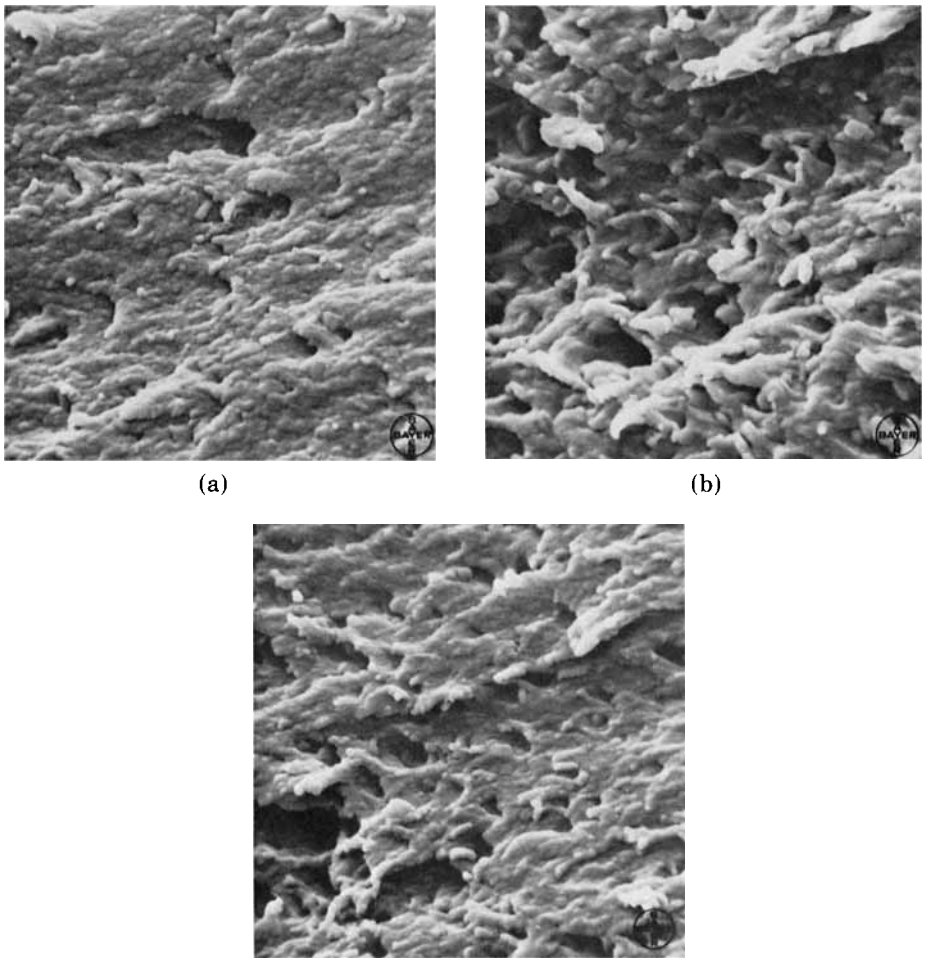

Fig. 13. (a)–(c) Scanning electron micrographs from the fracture surfaces as shown in Fig. 12, but at low strain rate. Magnification 5000×.

LPLG material. A very characteristic point is the decrease in residual strain and the decrease in force rise beyond the yielding. A mass–bead–ABS as a fourth material is added in Figure 15; it has a particle size much larger than the LPHG material and fits very well into the scheme of Figure 15. The cause for the different behavior of the materials in Figure 15 is the change in deformation mechanism characterized by the transition from shear yielding to crazing as preferential deformation mode if the particle size is increased. It is clear that this correlation holds only if additional parameters such as strain rate, grafting, and crosslinking and the structure of the matrix resin are taken into account.

Finally, Figure 16 gives a transmission electron micrograph of a crazed section of a SPHG/LPLG sample from the notched impact test which has been prepared by Kato's method. It is clearly visible that craze initiation is established mainly by the large particles. These are embedded in a resin matrix

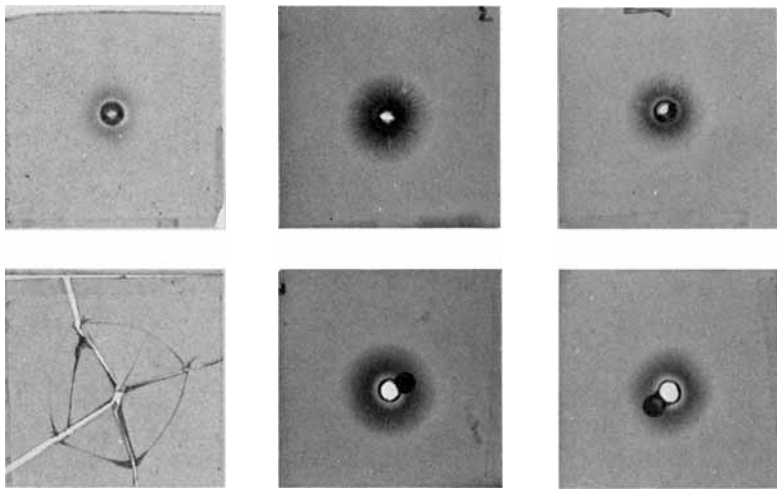

Fig. 14. Penetration of thin plates at low (top) and high (bottom) strain rate for SPHG (left), LPLG (middle), and SPHG/LPLG (right) with 17.5% rubber.

which must be regarded as modified in a certain way (localized crosslinked) by the small-particle component. This modified resin offers additional deformation characteristics and may also serve as a dispersing agent for the large particles. The statistical arrangement of the small particles must influence the craze-propagation stage as each craze, once started by a large particle, tends to follow up traces in the modified resin where the modulus is locally lowered by the presence of the small particles. The craze bands may have a tendency for branching, and they will often follow slightly curved traces.

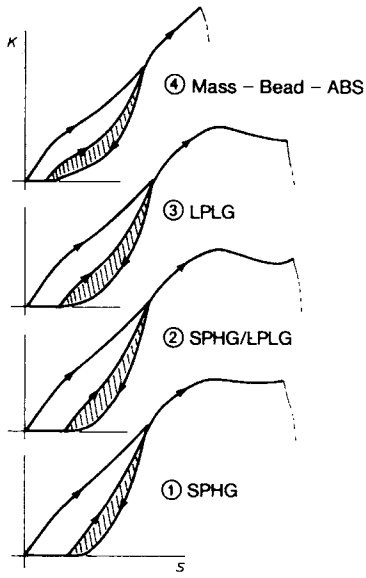

Fig. 15. Force–deformation curve from penetration test at low strain rate for SPHG, SPHG/LPLG, LPLG, and a mass–bead material; low strain rate; 17.5% rubber (1–3).

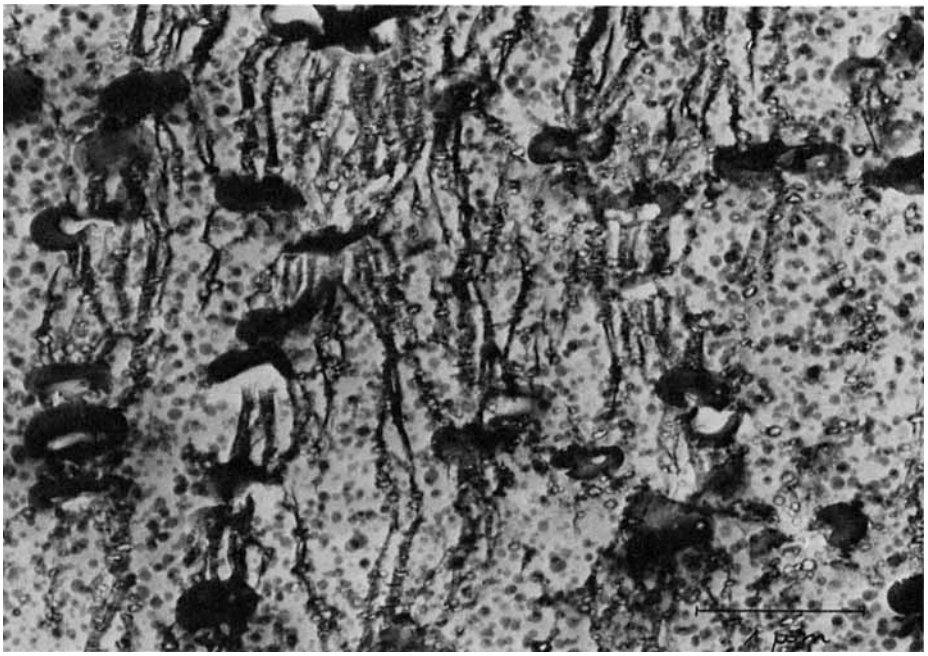

(a)

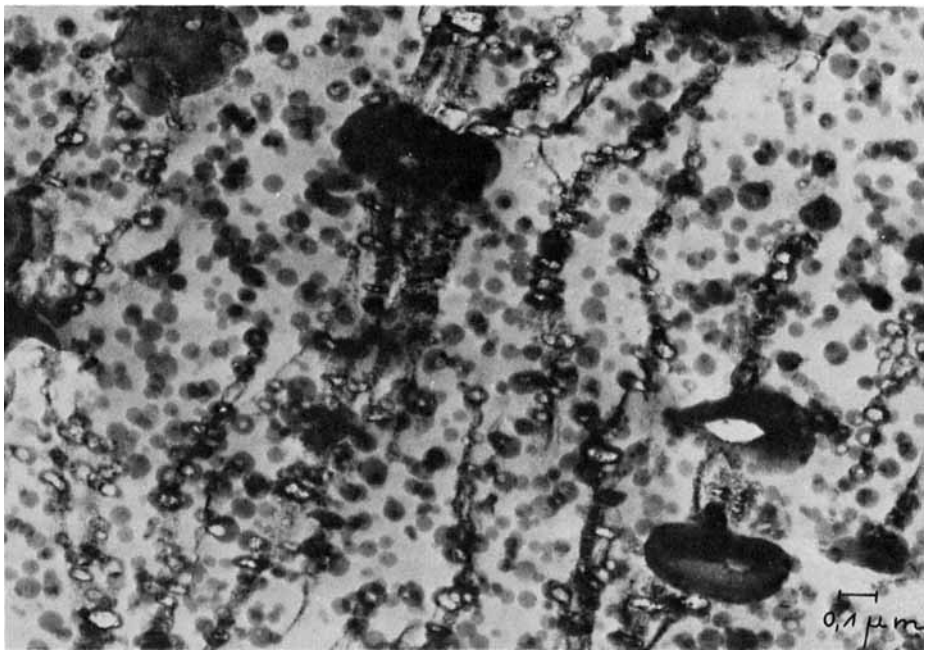

(b)

Fig. 16. (a) and (b) Transmission electron micrograph from the crazed region of the SPHG/LPLG material (notched impact; 12.5% rubber).

The small particles, therefore, behave as a reinforcing element within the crazed material whereby their high grafting degree becomes very important. This may be responsible for the relatively good toughness at lower temperature. The large-particle component has a lowered craze initiation stress, which may be a reason for the onset of crazing in a larger sample volume. The low grafting degree of the large particles will lead to an inhomogeneous grafting shell which, on the other hand, favors craze initiation simultaneously at different sites in the phase boundary; this can be seen in Figure 16. A high degree of grafting will restrict craze initiation to the equator plane of the particle. The presence of the small particles will influence the yield process to the effect that shear deformations may occur to a certain extent in addition to crazing. Both deformation modes can interfere in a positive way.[12]

CONCLUDING REMARKS

Further work will be done in quantifying the above discussed results and in answering some refined questions concerning the role of the grafting parameter, i.e., number, length, and length distribution of grafted chains and the chemical structure of the grafted chains. It may be pointed out that the structure of the graft shell of the large particles in the bimodal/bigraft systems is very influential. It is significant that good impact properties of this system are attainable with grafting parameters of the large particles which do not succeed so well in the usual large-particle system.

The authors would like to acknowledge the laboratory assistance of U. Brenneisen, J. Faehndrich, and H. Palla as well as the performance of transmission electron micrographs by G. Kämpf and the many discussions by H. Hespe.

References

1. E. Dinges and H. Schuster, *Makromol. Chem.*, **101**, 200 (1967).
2. M. R. Grancio, *Polym. Eng. Sci.*, **12**, 213 (1972).
3. M. R. Grancio, A. A. Bibeau, and G. C. Claver, *Polym. Eng. Sci.*, **12**, 450 (1972).
4. J. N. Sultan and F. C. McGary, *Polym. Eng. Sci.*, **13**, 29 (1973).
5. C. F. Pearsons and E. L. Suck, *Advan. Chem. Ser.*, **99**, 340 (1971).
6. R. H. Beck, S. Gratch, S. Newman, and K. C. Rusch, *Polym. Lett.*, **6**, 707 (1968).
7. J. Paterno, L. Ongchin, and S. Sternstein, IUPAC Symposium, Leiden, 1970.
8. L. Bohn, *Angew. Makromol. Chem.*, **20**, 120 (1971).
9. L. Morbitzer, K. H. Ott, H. Schuster, and D. Kranz, *Angew. Makromol. Chem.*, **27**, 57 (1972).
10. L. Bohn, *Angew. Makromol. Chem.*, **29/30**, 25 (1973).
11. L. Morbitzer, K. H. Ott, H. Schuster, and R. Bonart, *Angew. Makromol. Chem.*, **14**, 147 (1970).
12. C. B. Bucknall and D. Clayton, *J. Mat. Sci.*, **7**, 202 (1972).
13. C. B. Bucknall, II. International Conference on Yield, Deformation and Fracture, Cambridge, 1973.
14. R. P. Kambour, *J. Polym. Sci., Macromol. Rev.*, **7**, 1 (1973).

Received October 20, 1975
Revised December 26, 1975